ACS OMEGA

http://pubs.acs.org/journal/acsodf
Article

Electric Polarization-Dependent Absorption and Photocurrent Generation in *Limnospira indica* Immobilized on Boron-Doped Diamond

Nikolay Ryzhkov,* Nora Colson, Essraa Ahmed, Paulius Pobedinskas, Ken Haenen, Artur Braun,* and Paul J. Janssen

Cite This: *ACS Omega* 2024, 9, 32949−32961

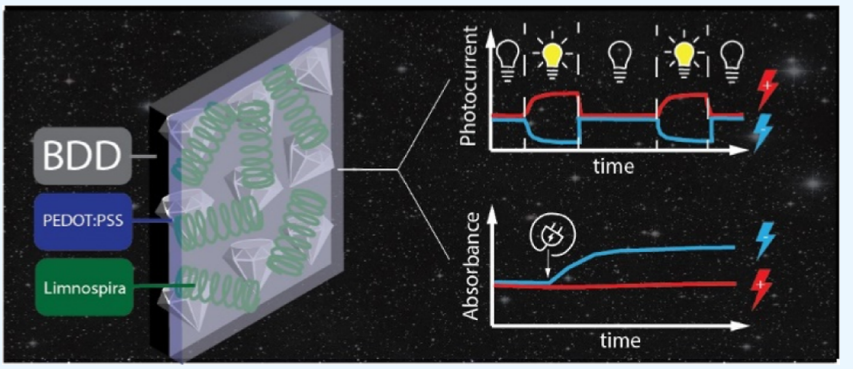

ABSTRACT: We present the change of light absorption of cyanobacteria in response to externally applied electrical polarization. Specifically, we studied the relation between electrical polarization and changes in light absorbance for a biophotoelectrode assembly comprising boron-doped diamond as semiconducting electrode and live *Limnospira indica*PCC 8005 trichomes embedded in either polysaccharide (agar) or conductive conjugated polymer (PEDOT−PSS) matrices. Our study involves the monitoring of cyanobacterial absorbance and the measurement of photocurrents at varying wavelengths of illumination for switched electric fields, i.e., using the bioelectrode either as an anode or as cathode. We observed changes in the absorbance characteristics, indicating a direct causal relationship between electrical polarization and absorbing properties of *L. indica*. Our finding opens up a potential avenue for optimization of the performance of biophotovoltaic devices through controlled polarization. Furthermore, our results provide fundamental insights into the wavelength-dependent behavior of a bio photovoltaic system using live cyanobacteria.

INTRODUCTION

The use of living organisms for conversion of solar energy to value-added products through the process of photosynthesis is an exciting field of research that has regained interest recently.[1,2] Photosynthetic organisms, particularly algae and cyanobacteria, can be deployed on various scales to generate electricity,[3] produce biofuels,[4] synthesize valuable compounds,[5] or drive other electrochemical reactions, including those for biosensing,[6] depending on the specific biological components and electrode materials used. Since biophotoelectrochemical cells (BPECs) utilize the natural process of photosynthesis and maintain their performance as long as a stable provision of photonic energy of adequate wavelength and necessary nutrients is guaranteed, they are considered for integration into regenerative life support systems (closed-loop systems), such as those used in space exploration or other harsh environments like deserts.[7,8] BPECs and larger bioreactors in space can generate electricity while recycle carbon dioxide, generate oxygen and biomass to be utilized either as supplementary food,[9] biofertilizer[10] or as construction material (in the form of biopolymers), and a range of biofuels and chemical products in the context of in situ resource utilization,[11] contributing to durable self-sustaining environments for space travel and colonization.[7,12]

BPECs can make use of intact microorganisms or photosynthetic components extracted from them.[13] Either way, the current density output of such BPECs is typically in the low mA/cm^2 range.[14] In particular, devices containing intact cells produce low to very low current outputs up to 1 mA/cm^2.[14] A 100 μA/cm^2 current density is considered to be indicative for

Received: April 24, 2024
Revised: June 21, 2024
Accepted: June 28, 2024
Published: July 17, 2024

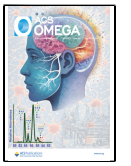

an enhanced biophotoelectricity generation.[15] Since there is a physical barrier that constrains, or impedes the charge transport between the photosynthetic component and the typically inorganic current collector, the use of certain chemicals as redox mediators is widely practiced.[16] Nevertheless, BPECs are seen mainly as instruments for sustainable energy generation in niche applications rather than that for high-power electricity generation. Using living cells can thereby be beneficial in terms of their ability to overcome and adapt to changing environmental conditions, providing functionality for extended periods of time.[17] Additionally, different microorganisms have unique metabolic pathways and capabilities, allowing in principal for the production of a wide range of valuable products depending on the chosen microorganism.[18] Other important features of living photosynthetic microorganisms are that they can generate current under light and dark conditions via photosynthetic and respiratory systems, respectively,[19] while they do not require the time and effort-consuming procedures of photosynthetic component extraction and purification.

Cyanobacteria, being prokaryotes, are the most preferable microorganisms used in this field because of their metabolic and physiological simplicity compared to eukaryotes, e.g., algae. One of the promising candidates for designing BPECs for space applications is *Limnospira indica* PCC 8005 (formerly known as Arthrospira sp. PCC 8005[20]) which has previously demonstrated reliability under harsh space conditions.[21]

Examples of utilizing both freely floating cells[22] and those deposited through gravity-induced deposition,[23] as well as immobilized cells[24] in BPECs, can be found in the literature. However, encapsulating cells in an immobilizing matrix attached to the current collector material can have several advantages. Such a biofilm-like architecture can protect cells from environmental stress[25] and help avoid certain scalability issues and limitations in precision electrode engineering. Good connectivity between cells embedded in the matrix and immobilized on top of the current collector allows for faster electron transfer.[26] Such compact and dense quasi-biofilm architecture of the cells increases the number of cells that are in close contact with the current-collecting material, resulting in higher photocurrent as compared to cyanobacterial suspensions. The 3D-bioprinting presents a promising technique to cultivate immobilized cyanobacteria and microalgae.[27] Due to their high water content and ability to facilitate exchange of gas, nutrient, and charge mediator, hydrogels are a suitable material for immobilizing cyanobacteria.[28] An algal-alginate biofilm within a biophotovoltaics (BPV) device demonstrated a maximum power density output (obtained by multiplying current density to corresponding potential) of 0.289 mW/m^2, which is 18% higher compared to the conventional suspension culture BPV.[29] The BPV performance is based on phenomena of extracellular electron transport (EET), a biological process in which microorganisms, such as bacteria, transfer electrons from the cell interior to external electron acceptors, typically located outside the cell. Given that cyanobacteria predominantly depend on photosynthesis for their primary energy source, the extent of EET in these photosynthetic organisms is generally limited when compared to other bacterial species. Various strategies can be employed to enhance electron transport between cyanobacteria and the current collector.[30] These strategies include using shuttling molecules[31] or a conductive polymer matrix to establish mechanical contact between redox-active outer-membrane proteins (e.g., c-type cytochromes) and the electrode material.[32]

Besides the photosynthetic components (biological cells) and the supporting matrix, another crucial component in a BPEC is the current-collecting material. Current collectors must meet several criteria, most important the good charge transfer across the bioelectronic interface,[2] but also biocompatibility, suitability for cell adhesion, and also, affordability. Many carbon allotropes are considered ideal candidates for this purpose, including diamond and diamond like carbon. Among them, boron-doped diamond (BDD) has garnered significant interest. Boron doping substantially enhances the electronic conductivity of diamond, making BDD electrodes effective current collectors. BDD benefits from a large band gap (5.47 eV), which is known for its wide electrochemical potential window of 3−3.5 V[33] and does not release any toxic substances that could affect the biological components.[34] In addition, its electrochemical properties are tunable by the boron concentration in the diamond lattice, presence of sp^2 carbon, and surface termination,[35] low background current, and significant chemical inertness.[36]

The production of photocurrent in a BPEC depends on the applied potential bias. Optimizing the applied potential can significantly improve the performance of the BPEC. For photoelectrodes where photosystem I (multisubunit enzyme that uses light energy to catalyze the transfer of electrons across the thylakoid membrane where light-dependent reactions occur) is utilized, potentials lower than the open-circuit potential (OCP) lead to an increase in cathodic photocurrent. At the potential ranging from approximately +200 to +400 mV vs OCP, the photocurrent was close to zero, while at higher potential, anodic photocurrent was measured.[37] Thylakoid-based devices demonstrated anodic photocurrents at positive polarization, reaching saturation at +0.5 V vs Ag/AgCl.[38]

Apart from electric role in electron extraction, polarization may influence cell behavior and, consequently, photosynthesis. Drastic changes like the reversal of an electric field could impact the properties of cell membranes,[39] including the electrochemical gradients across thylakoid membranes[40] within cyanobacterial cells, or potentially disrupt the structure and function of the photosynthetic machinery within these cells.[41] Unfortunately, this aspect has not been systematically studied so far and remains poorly documented in the literature. Enhanced release of nicotinamide adenine dinucleotide phosphate (NADPH), which is a reducing agent for biosynthetic reactions and protector against toxic reactive oxygen species (ROS), has been observed in cyanobacteria and microalgae when living cells were associated with the anode of a BPEC and an electrical bias potential was applied.[42] It was demonstrated that electric pulse fields can generate membrane potential, leading to change in activation energy of reactions in the photosystem resulting in delayed fluorescence and fluorescence yield decrease.[43] Furthermore, changes in electrical potential may influence gene expression, although short-term changes in electrical potential do not appear to affect microorganisms.[44] External electrical polarization can also impact the oxidation state of cytochrome c, an essential molecule of the electron transport chain.[45]

The technological focus of bioelectrochemistry research directed toward the design of BPECs is to achieve a maximum conversion efficiency and to obtain the highest current outputs possible by optimizing the EET. However, it is essential to

https://doi.org/10.1021/acsomega.4c03925
ACS Omega 2024, 9, 32949−32961

recognize that pursuing the highest efficiency may not necessarily be the best choice for long-term autonomous operation since, as outlined above, electric fields may affect metabolic or enzymatic processes that are vital for cyanobacteria.

Unlike inanimate photoelectrochemical systems, those based on living organisms involve a multitude of chemical reactions and metabolites that take place within the cells. While biophotoelectrochemistry is a well-developed field of science, with comprehensive research on the photosynthesis process and its application in electricity and fuels production, there are still numerous factors that are difficult to control in experiments or even to observe separated simultaneously.

Another factor limiting photosynthetic efficiency is the saturation of the photosynthetic apparatus, often due to the reduction of electron carriers like plastoquinone. Consequently, polarization by external bias, leading to oxidation or reduction processes, can influence the overall photosynthetic efficiency. Furthermore, a reduction in electron-transfer intermediates may result in the additional generation of harmful ROS.[46]

In this study, we investigated the effect of electrochemical polarization on a biophotoelectrode containing intact, living cyanobacterial cells on their light absorption capability and photocurrent production. Our focus was to understand how this electrochemical modulation influenced the light absorption capabilities of the studied cyanobacterium *L. indica* and subsequently affected the production of photocurrent when exposed to monochromatic light.

MATERIALS AND METHODS

Diamond Electrode Preparation. BDD thin films were coated on 40 mm × 10 mm fused silica substrates. Prior to the thin-film deposition, the substrates were cleaned using an O_2 gas discharge plasma following the method outlined in a ref 47. Substrates were then seeded by drop-casting with a water-based colloidal suspension of ultradispersed detonation nanodiamond of size 7 nm followed by deionized water rinsing and spin-coater drying.

Diamond growth was carried out in an ASTeX 6500 series microwave plasma-enhanced chemical vapor deposition reactor. The BDD film growth process was performed in a CH_4/H_2/trimethylboron (TMB) plasma, with corresponding gas flows of 5/395/100 standard cubic centimeters per minute (sccm) that result in methane concentrations of 1% and a B/C ratio of 20,000 ppm (TMB gas is diluted to 1000 ppm in H_2). The microwave power and pressure were set to 4000 W and 40 Torr, respectively. The substrate temperature, monitored using a portable pyrometer, was maintained at 730 °C. The resulting thickness of the film was 180 nm.

Cyanobacteria Cultivation. Axenic cultures of *L. indica* PCC 8005 of helical trichome morphotype (P6)[48] obtained from SCK CEN (Mol, Belgium) were grown in 200 mL of Zarrouk's medium[49] of optimized composition[50] in 550 mL cell culture flasks (CELLSTAR, Greiner Bio One, Austria) at a constant temperature of 30 °C in an orbital shaker-incubator ES20/60 (Biosan, Riga, Latvia) at 100 rpm and 0.5 mW/cm^2 white light illumination produced by a light-emitting diode (LED) strip. An aliquot of approximately 24 mL was taken and distributed in small 2 mL centrifuge tubes. Cyanobacteria were harvested by 1 min of centrifugation at 9000 rpm (5430*g*) using IKA G-L centrifuge.

Biophotoelectrode Assembly. Harvested *L. indica* PCC 8005, helical P6 morphotype, were resuspended at 1:1 v/v in 0.75% agar (05040, Millipore, melted, 50 °C) or 0.5−1% PEDOT/PSS in water (Sigma-Aldrich). The agar used in this study contained, where noted, also 100 mM $[Fe(CN)_6]^{3+}$ as a redox mediator. Thus, obtained BDD electrochemically tested sample surfaces were limited to approximately 1 cm^2 by blanking off the rest of the specimen area using Lacomit varnish (Agar Scientific, Stansted, UK). Bacterial cell suspensions were drop-cast on the surface of BDD electrodes. The obtained biophotoelectrodes are denoted as BDD/agar + P6 and BDD/PEDOT−PSS + P6 further in the text. In current density calculations, the exposed area of 1 cm^2 were used even though real surface area can be different due to different polymer-embedded cyanobacteria layer micromorphology.

Cyanobacteria Viability Test. Embedding in a polymeric matrix may be a stress factor to cyanobacteria, particularly when using hot agar. Hence, we studied their viability (i.e., *L. indica* PCC 8005, helical trichome morphotype, and substrain P6) after contact with polymer by transferring 200 μL of cell suspension in agar or PEDOT/PSS (1:1 v/v) into 20 mL of Zarrouk's medium for renewed cultivation under the same conditions as described above. Cell growth was monitored daily by measuring absorption of cyanobacteria suspension at 440, 555, 635, and 687 nm corresponding to chlorophyll b (Chl b), phycoerythrocyanin (PEC), phycocyanin (PC), and chlorophyll a (Chl a), respectively, using a SEC2000 UV−vis spectrometer (ALS Electrochemistry & Spectroelectrochemistry, ALS Co., Ltd., Tokyo, Japan). Optical microscopy images were recorded using a Motic AE2000 microscope (Motic Europe, Barcelona, Spain) with 20× objective.

Light Absorbance vs Polarization Measurements. The light harvesting ability of cyanobacteria under electric polarization was measured in situ using a spectroelectrochemical cell SEC-C (ALS Electrochemistry & Spectroelectrochemistry, ALS Co., Ltd., Tokyo, Japan) with a SEC 2000 spectrometer system of the same manufacturer utilizing a deuterium and tungsten halogen lamp. Cyanobacteria embedded in agar or in the PEDOT/PSS matrix were deposited on a gold gauze electrode used as the working electrode in a three-electrode electrochemical setup, together with a Pt-counter electrode and an Ag/AgCl reference electrode in PBS solution (0.01 M phosphate buffer, 0.0027 M potassium chloride, and 0.137 M sodium chloride, Sigma-Aldrich). The transients of absorption at +0.6 and −0.6 V applied DC bias were monitored.

Photocurrent Measurements. Photocurrents produced by BDD/agar + P6, BDD/PEDOT/PSS + P6, and blank photoelectrodes of the same composition but with no cyanobacteria under illumination were measured by a Gamry Interface 1010E potentiostat (Warminster, USA) in a three-electrode setup with a Pt counter electrode and an Ag/AgCl reference electrode. Measurements were performed in a single custom-made single compartment electrochemical cell with an optically transparent quartz window allowing the exposure of the working biophotoelectrode. During chronoamperometry measurements, the biophotoelectrode was periodically exposed to monochromatic light from mounted LEDs (Thorlabs, Newton, USA; specification see below). Approximately 1 min of illumination was followed by 1 min in darkness. Steady-state dark current values were extrapolated for the entire time of the chronoamperometric measurement. This extrapolated dark current curve was used as a baseline and subtracted from the measured curve to obtain the photocurrent curve.

https://doi.org/10.1021/acsomega.4c03925
ACS Omega 2024, 9, 32949−32961

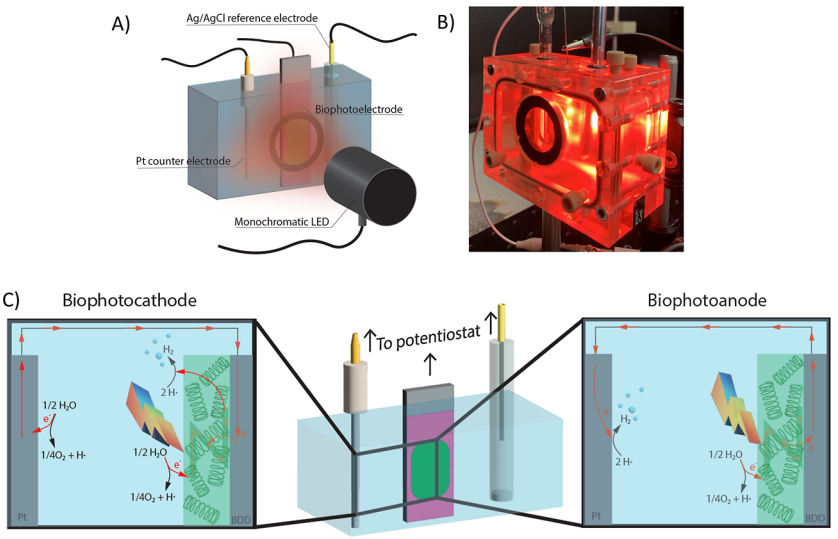

Figure 1. (A) Experimental setup of our three-electrode electrochemical cell: a working biophotoelectrode made of BDD substrate onto which cyanobacteria were immobilized, an Ag/AgCl reference electrode, and a Pt counter electrode; the biophotoelectrode is exposed to light through a quartz window; (B) photograph of the electrochemical cell illuminated by red light at 625 nm; and (C) scheme of electron flow in our experimental BPEC when the biophotoelectrode is used as a biophotocathode (on the left) or as a biophotoanode (on the right).

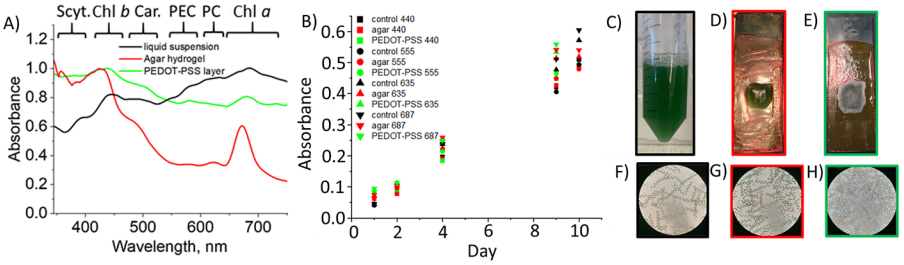

Figure 2. (A) UV−vis light absorption spectra of liquid cyanobacteria suspension and cyanobacteria suspended in agar hydrogel and PEDOT/PSS, Scyt—Scytonemin, Chl a—chlorophyll a, Chl b—chlorophyll b, Car—carotenoids, PEC—phycoerythrocyanin, and PC—phycocyanin, spectra are normalized with respect to their maximum absorbance within wavelength range presented. (B) Evolution of the light absorption ability of *L. indica* cells inoculated from matrix-free control culture, a mixture of *L. indica* cells with hot agar (we recall, above its melting point, around 50 °C) and a mixture of *L. indica* cells with PEDOT/PSS. This graph shows the time evolution of absorbance for the main absorption bands at 440 nm (Chl b), 555 nm (PEC), 635 nm (PC), and 687 nm (Chl a). (C) *L. indica* matrix-free control culture. (D) Cyanobacteria in agar hydrogel on top of the BDD electrode. (E) Cyanobacteria in PEDOT/PSS on top of the BDD electrode. (F−H) Optical microscopy images of cyanobacteria after 10 days of cultivation in Zarrouk medium. (F) Free floating cyanobacteria in matrix-free Zarrouk medium. (G) Cyanobacteria-hot agar suspension. (H) Cyanobacteria-PEDOT/PSS suspension.

Illumination was provided by the LEDs with wavelengths 375 nm (M375L4, full width at half maximum, fwhm 9 nm), 420 nm (M420L4, fwhm 14 nm), 470 nm (M470L4, fwhm 28 nm), 505 nm (M505L4, fwhm 37 nm), 530 nm (M530L4, fwhm 35 nm), 590 nm (M590L4, fwhm 15 nm), 625 nm (M625L4, fwhm 17 nm) (Thorlabs, Newton, USA). Depending on the wavelength of the LED, their intensity, respectively, the power density varied from 8 to 35 mW/cm^2. During the measurements, the current passing through the LED was controlled. The light intensity was measured using a S120VC Si photodiode detector and a PM100USB power and energy meter (both from Thorlabs). Photocurrent values were normalized to light intensity or photon flux and, when mentioned, to the amount of photons calculated as emitted light power divided by the energy per photon (Planck's constant times the frequency).

RESULTS AND DISCUSSION

Biophotoelectrodes. BPECs were constructed with a bioanode, a platinum counter electrode, and an Ag/AgCl reference electrode. The light-sensitive component of the anode consisted of intact live *L. indica* PCC 8005 cells. The anode current collector material consisted of BDD deposited on a fused-silica substrate. BDD served as a solid substrate for microbial attachment and as an electrical conductor for charge transfer (Figure 1A,B).

Ideally, immobilization should preserve cell viability and metabolic activity (sustained via photosynthesis when using phototrophs) at high cell densities while minimizing the loss of cells by detachment from the matrix. To achieve this, the immobilizing matrix should meet several criteria: it should be nontoxic, appropriately transparent, chemically stable when exposed to growth media, and mechanically robust.

Despite the potential unfavorable effects of immobilization procedures on light transfer,[51] our focus here is on immobilized cyanobacteria. This focus is driven by the importance of electrochemically connecting bacteria to the electrode for efficient charge transfer. Additionally, many cyanobacteria including *L. indica* are robust organisms often able to adjust their cellular machineries to stressful conditions.

https://doi.org/10.1021/acsomega.4c03925
ACS Omega 2024, 9, 32949−32961

Hence, we considered the direct impact of immobilization on the photosynthetic apparatus itself, i.e., inside healthy cyanobacteria, as negligible.

Cyanobacteria were deposited on the BDD electrode surface. We used two alternatives for immobilization: (i) an agar hydrogel and (ii) a PEDOT/PSS layer. The choice of agar is based on its ability to form stiff hydrogels that strongly adhere to the surface, whereas PEDOT/PSS is chosen for its properties as a translucent conductive polymer.[52,53]

The procedure for cyanobacterial immobilization involves adding a concentrated cell suspension to hot agar (above its melting point, around 50 °C). Although high temperatures are typically considered a stress factor for bacteria, the limited exposure time during which the agar cools down and gelates and the intrinsic resistance of *L. indica* PCC 8005 to adverse environmental conditions suggest that cell viability on the whole would not be affected. In addition, PEDOT/PSS has previously been reported to be fully biocompatible.[54]

Light absorption spectra of cyanobacteria in a liquid suspension and cyanobacteria immobilized in both agar and PEDOT/PSS were determined (Figure 2A). While the baseline of the spectrum for the liquid suspension differs, and the intensity of absorption bands varies significantly, all spectra exhibit the same absorption features at the same wavelengths: 364 nm (scytonemin), 430−440 nm (Chl b), 525 nm (carotenoids), 555−560 and 580 nm (PEC), 635 nm (PC), and 660 and 687 nm (Chl a). These absorption bands have been identified based on literature data.[55,56] It is worth noting that pigments absorbing in the blue-green part (400−525 nm) of the spectrum may not always appear as separate peaks.[56]

To evaluate whether immobilization procedures have a negative effect on the normal growth and function of *L. indica*, we recultured cell suspensions in hot agar and PEDOT/PSS in fresh Zarrouk medium. The initial cell concentrations across these cultures were approximately equal. 24 h after inoculating fresh Zarrouk's medium with cyanobacteria suspension, agar, or PEDOT/PSS-embedded cyanobacteria, various absorption bands were discernible at the wavelengths mentioned above (Figure 2B). Additionally, we observed that the absorbance for cultures inoculated from cyanobacteria exposed to hot agar and PEDOT/PSS was higher compared to the control culture inoculated with cyanobacteria suspension in water. In the subsequent days, absorbance levels varied, with the control culture or cultures inoculated from agar or PEDOT/PSS-exposed cyanobacteria sometimes having higher absorbance values (Figure S1A−C). Nevertheless, the general trend of absorbance increase was consistent among all cultures, indicating that the interaction with hot agar or the conductive polymer had little or no influence on the reproductive ability and viability of the cyanobacterial cells. Since chlorophyll, PC, and PEC are a good proxy for cyanobacterial biomass,[57] changes in absorbance over time at 440 and 687 corresponding to chlorophylls and 555 and 635 corresponding to, respectively, PEC and PC were monitored for *L. indica* PCC 8005 recultured from cells immobilized in agar, PEDOT/PSS, and a control culture (Figure 2B)—a detailed resolution of the spectral features can be found in the Supporting Information file (Figure S1D−F). Some shifts in peak positions were observed on the eighth day. For example, the absorption band at 660 nm shifted to lower wavelengths, and in general, absorption bands in the green-red part of the spectrum became more complex to distinguish. However, these shifts were consistently observed across all cultures studied in this experiment.

L. indica trichomes in the matrix-free control culture or in the immobilized form displayed a healthy green color (Figure 2C−E). Also, optical micrographs of different representative samples demonstrated that the immobilization procedures we deployed did not negatively affect the filamentous structure and physical integrity of the studied *L. indica* cells (Figure 2F−H).

Based on these results, we concluded that *L. indica* cells embedded in agar or PEDOT/PSS matrices were unaffected in growth.

Biophoto-Electrode Light Absorption Dependence on Potential Bias. Oxygenic photosynthesis is a vital process that sustains life on Earth by generating oxygen (i.e., using water as electron donor) and producing energy-rich molecules crucial for the growth and metabolism of cyanobacteria, algae, and plants. Our interest here is primarily on the light-dependent processes that occur in the thylakoid membranes of the cyanobacterium *L. indica*. These processes involve multiple steps, including the absorption of light energy by chlorophyll and other pigments, liberation of protons (H^+) and electrons (e^-) from water while evolving oxygen (the "splitting" of water molecules), the transfer of electrons through a series of protein complexes, and the formation of the energy storage molecule adenosine triphosphate (ATP) and the reduced electron carrier NADPH.[58]

In essence, the photosynthesis process involves a sequence of oxidation and reduction reactions that facilitate the transfer of electrons from oxidized water molecules to ATP and NADPH. As previously demonstrated, maximum photocurrent values were achieved at positive potential bias (e.g., +0.6 V). However, electric polarization can influence the electron transport chain, a crucial component of the photosynthetic process.[59] Our experimental setup consisted of a BPEC composed of a working biophotoelectrode of immobilized *L. indica* on BDD (connected as a cathode or an anode) and a Pt counter electrode, with electrochemical measurements at different external potential biases (Figure 1C). While this scheme does not take into account complex processes within photosynthetic cells, it clearly demonstrates how photosynthetic activity can be utilized for the production of electric current and valuable biochemicals (Figure 1C demonstrates hydrogen production but depending on system materials and -setup, as well as choice of organism, substrate, and mediator, BPECs are applicable in a wide range of solar-to-chemical productions).

When comparing the absorption of cyanobacteria embedded in agar and PEDOT/PSS (Figures 2A and S2A), a shift of Chl a and Chl b peaks can be noted (Figure S2B) with short wavelength peak (Chl b) shifts from 426 to 437 nm and long wavelength peak (Chl a) shifts from 670 to 680 nm. The PEC peak is much better pronounced for cyanobacterial cells embedded in conductive PEDOT/PSS as compared to PEC profiles for cells in agar; however, the position of the PEC peak remains unchanged. In fact, the PC peak was clearly discernible as a shoulder to the PEC peak in absorbance profiles for *L. indica* in the PEDOT/PSS matrix but appears as a separate peak for agar hydrogel-embedded cyanobacteria (Figure S2A). Also, a shift of the carotenoid absorption band position can be seen from the second derivative of the absorption spectra (Figure S2B). Additionally, a small peak in the infrared part of the spectrum, which may correspond to phytochrome A, is

https://doi.org/10.1021/acsomega.4c03925
ACS Omega 2024, 9, 32949−32961

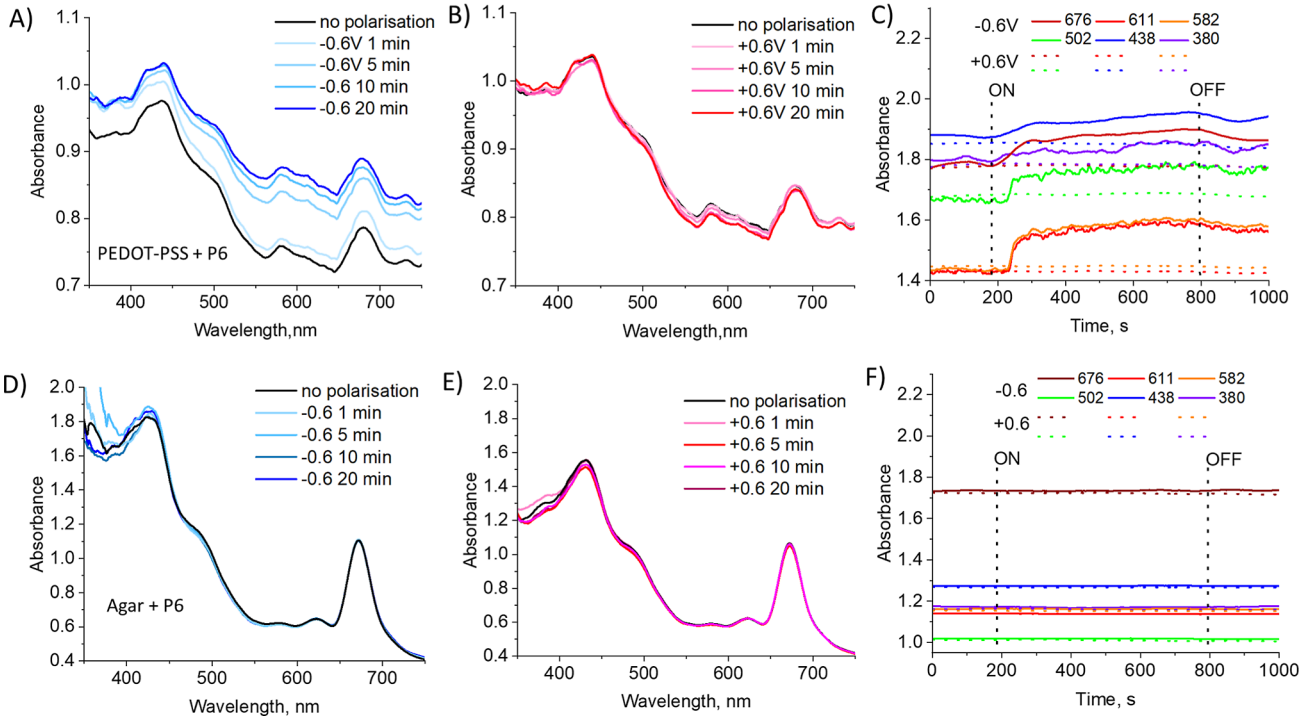

Figure 3. Differences in *L. indica* absorption spectra depending on polarization bias under various conditions. In conductive PEDOT/PSS polymer (A–C) under applied potential bias: (A) −0.6 V vs Ag/AgCl, (B) +0.6 V vs Ag/AgCl, (C) with time-evolved absorbance of PEDOT/PSS-embedded cyanobacteria at main absorbance bands and the timing of ON/OFF switching of polarization bias; solid line, negative bias; dotted line, positive bias. In agar hydrogel (D–F) under applied potential bias: (D) −0.6 V vs Ag/AgCl, (E) +0.6 V vs Ag/AgCl, and (F) time-evolved absorbance of agar hydrogel-embedded cyanobacteria at main absorbance bands with the time of switching on and off of polarization bias.

present in the spectrum obtained for PEDOT/PSS-embedded cells and liquid suspension (Figure 2A) but not for agar-embedded cells. A possible explanation is that phytochromes are known to be thermosensitive,[60] and the procedure of embedding cyanobacteria into an agar gel assembly requires a melting temperature over 50 °C. An effect of absorbance peak shifting induced by an external electric field was reported for extracted chloroplasts and explained by polarization and changes in the orientation of Chl a and carotenoids.[61] Even though these data were obtained for cyanobacteria embedded in different polymer matrices but with no external field applied yet, this absorption shift can be attributed to self-bias emerging due to the interaction with conductive and electrochromic polymers. Changes in light absorption spectra over time under applied electric polarization bias are depicted in Figure 3 for PEDOT/PSS (A,B) and agar (D,E)-embedded cyanobacteria. As can be seen from Figure 3, when cyanobacteria are embedded in a polymer matrix, they exhibit the main absorption features typical for cyanobacteria as reported before,[62] including chlorophyll absorption bands at 680–690 (Chl a) and 440 nm (Chl b), a wide absorption band corresponding to β-carotenes and PEC (appearing as a right shoulder to the Chl b peak), and a PC peak at 625–635 nm. When comparing the absorption of cyanobacteria embedded in agar and PEDOT/PSS, it is notable that higher absorption of yellow light (which can shift the PC peak) is observed in cells embedded in the conducting polymer. Additionally, a small peak is seen at wavelengths above 700 nm, which may originate from phytochrome A.

With respect to the baseline (no electric polarization), we observed an increase in PEDOT/PSS + P6 layer absorbance under reductive conditions—(−0.6 V vs Ag/AgCl polarization) (Figure 3A). An abrupt change in absorption corresponded to the moment when electric polarization was switched on (Figure 3 panel C, solid lines). However, changes in absorption in the green and red parts of the visible light spectrum show some delay compared to the blue, violet, and far-red regions. After switching off external polarization and allowing for relaxation under open-circuit conditions, there is a slight decrease in absorption, but it does not immediately return to the initial values, indicating a lasting effect of electric polarization or a delay in response (data were collected up to 200 s after polarization switch-off) (Figure 3C). Furthermore, no changes in the peak position were observed for spectra of the polarized biophotoelectrode in comparison to the spectra for nonpolarized biophotoelectrode (Figure S3).

In contrast, positive polarization did not lead to increase of absorbance at chosen wavelengths (Figure 3B). Spectroelectrochemical measurements of absorbance evolution for selected wavelengths (absorbance peak positions) do not indicate any significant response to electric polarization (Figure 3, panel C, dotted line).

Figure 3D–F demonstrates that similar phenomena are not observed for agar-embedded cyanobacteria probably due to low conductivity of agar hydrogel preventing any reduction/oxidation reaction or electric field influence. Figure S4A demonstrates charge flow through electrodes made of cyanobacteria-containing agar or -PEDOT/PSS as well as pure PEDOT/PSS when polarized. From this, we conclude that the electric conductivity of PEDOT/PSS-based electrodes is higher than as compared to agar-based electrodes. There is as well a significant positive contribution of cyanobacteria in the conductivity of cyanobacteria-containing polymeric matrices albeit more pronounced when PEDOT/PSS is used.

https://doi.org/10.1021/acsomega.4c03925
ACS Omega 2024, 9, 32949−32961

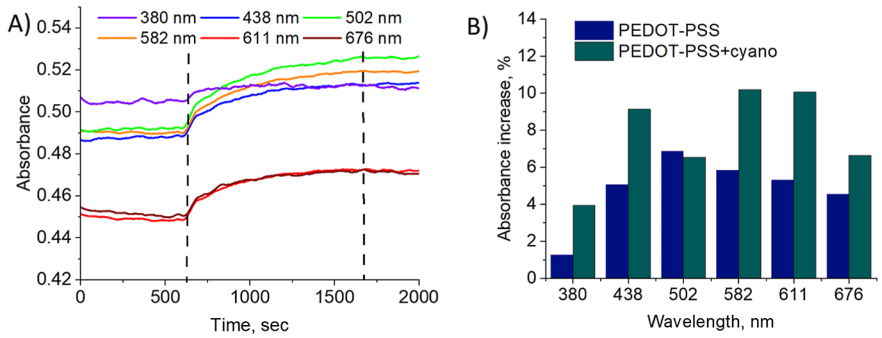

Figure 4. (A) Evolution of light absorption bands of PEDOT/PSS under −0.6 V potential bias, (B) comparison of the relative increase of absorption for PEDOT/PSS only and PEDOT/PSS containing cyanobacteria.

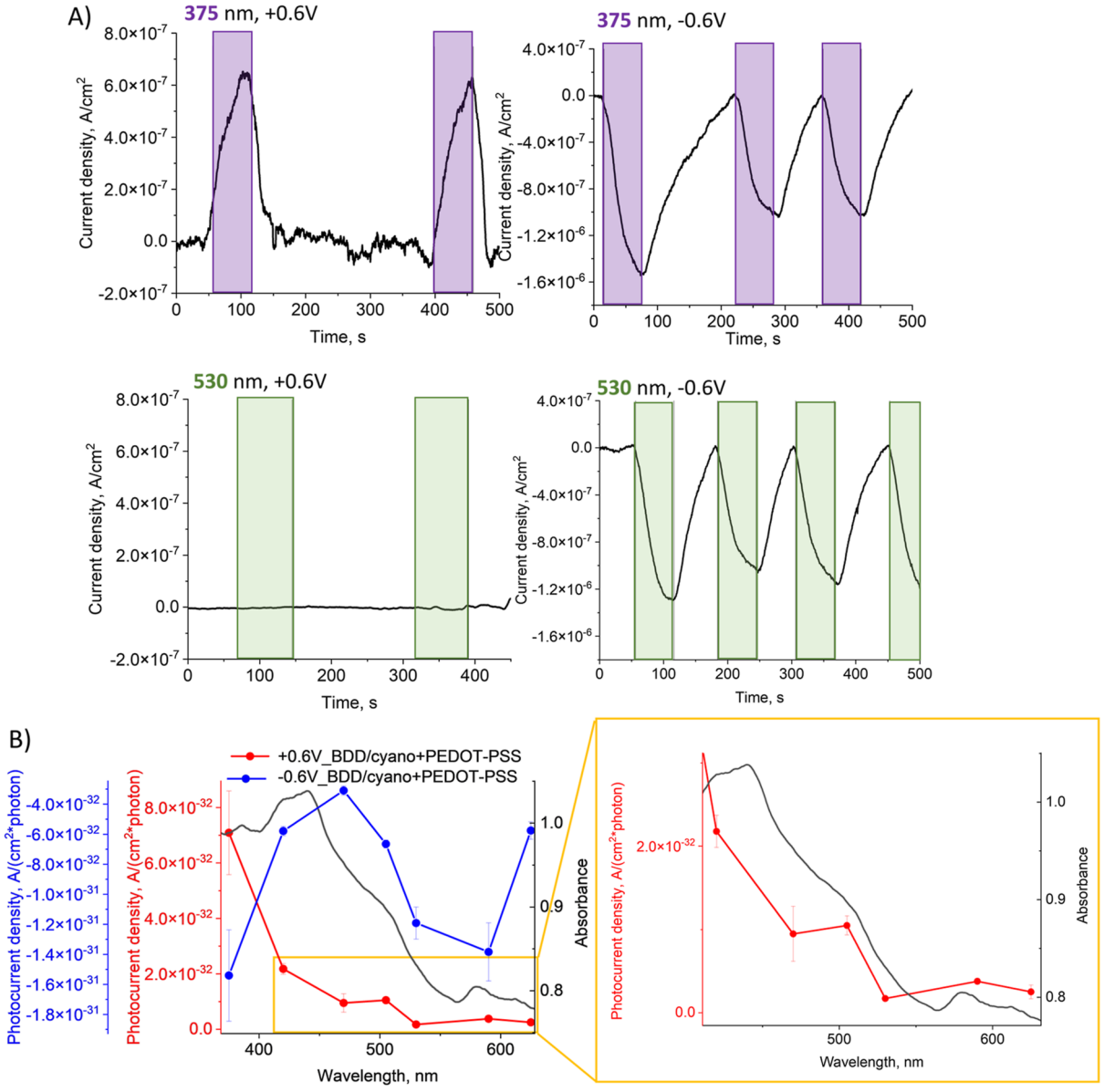

Figure 5. (A) Chronoamperometry curves for BDD/PEDOT/PSS biophotoelectrode with cyanobacteria. Colored bars designate periods of illumination by UV light (375 nm) and green light (530 nm) at applied potential biases of +0.6 and −0.6 V. (B) Steady-state photocurrents (extracted from chronoamperometry curves and normalized to photon flux) produced by the BDD/PEDOT/PSS biophotoelectrode with cyanobacteria under illumination by monochromatic light at applied potential biases of +0.6 and −0.6 V. These photocurrents are normalized to photon flux and plotted together with the absorption spectrum of BDD/PEDOT/PSS + P6 for reference.

https://doi.org/10.1021/acsomega.4c03925
ACS Omega 2024, 9, 32949−32961

Another feature that could explain the absorbance increase at reducing potential is the electrochromic behavior of PEDOT/PSS, which involves fast, real-time, and efficient reversible color changes due to redox processes under the influence of an electric field.[63]

In general, the pattern of absorbance changes for PEDOT/PSS and the same polymer with embedded cyanobacteria (PEDOT−PSS + P6) is similar (Figure 3A,B). Absorbance increases when polarization is switched on, followed by stabilization. There is almost no absorbance increase observed in the UV-A region of the spectrum (350 nm), but there is a nearly 8% increase for green light (502 nm), approximately 5% for other regions of the spectrum (red-orange and blue), and about 5−6% for far-red and blue light. For PEDOT−PSS + P6, there is an 11−12% increase in absorbance for the green-red part of the visible light spectrum, a 5−6% increase for far-red and blue light, and only around 3% for UV (Figure 4B).

As for the possible reasons that change the amplitude of the absorbance, but without a shift on the wavelength position, we consider following. Cyanobacteria have pigments embedded in their thylakoid membranes, which absorb light which provides the necessary energy for photosynthesis. Electrical polarization across the membrane can alter the membrane potential,[64] which may influence the orientation and spatial arrangement of proteins.[65] Changes in pigment orientation can affect how light is absorbed, potentially enhancing, or diminishing light absorption efficiency.[66−68] Such reorientation can change the effective concentration of pigments in specific orientations, affecting the overall absorbance without shifting the wavelength.

Electrical polarization is also closely related to the generation and maintenance of the proton gradient.[69] Changes in the proton gradient can impact the activity of photosystems and other components of the photosynthetic electron transport chain, potentially altering the overall efficiency of light absorption.[70]

Another noteworthy point is that switching off polarization for PEDOT−PSS coating does not lead to a further decrease in absorbance (Figure 4A). Although PEDOT−PSS electrochromic behavior is fully reversible, it requires opposite polarization to reverse its effects.

In contrast, the polarization effect on living cells can be reversed after polarization is released due to *L. indica*'s apparent ability to self-heal and maintain internal integrity. Therefore, the effect of a BDD/PEDOT/PSS + P6 absorbance change under electrical polarization cannot be fully attributed to the electrochromic properties of the polymer matrix.

Photocurrent Measurements. BDD is a wide band gap p-type semiconductor and is expected to exhibit cathodic photocurrent when illuminated with photons, respectively, radiation with wavelengths less than 250 nm corresponding to its ∼5.5 eV band gap.

When cyanobacteria are exposed to light, their pigments absorb photons, leading to the release of excited electrons. These electrons can then be harvested by the electrode surface to produce electrical energy. Therefore, photoinduced current generation increases under illumination and decreases in darkness due to the shutdown of light-driven electron transport.

BPECs are designed to operate under sunlight, which has a complex spectrum (between 200 and 2500 nm at sea level, with a wider spectrum including electromagnetic radiation below 200 nm—most of this is blocked by the Earth's atmosphere—and higher irradiance in space). In this study, the ability of *L. indica* to produce photocurrent was tested under different applied potential biases and illumination with monochromatic light of various wavelengths. With this approach, we set out to assess the contribution of different photosynthetic pigments to photocurrent generation, taking into account our observation that the absorption characteristics of *L. indica* changed with positive versus negative potential bias (electric polarization), and absorption bands showing different responses to this polarization, even though they all exhibited an overall trend of increased absorbance during a negative potential bias.

In BPEC, water is split by the cyanobacteria using sunlight in the anodic chamber, and the released electrons are then captured by the anode (via a diffusible redox mediator or by microbial surface redox proteins) and transferred to the cathode to drive the evolution of pure hydrogen.[71] Positive polarization is usually required to facilitate this process. However, biophotoelectrodes can also be utilized in cathodic processes.[72] Arthrospira (Spirulina platensis) can produce hydrogen under complete anaerobic and dark conditions.[73] In general, cyanobacteria use nitrogenase and hydrogenases to generate hydrogen gas.[74] In the presence of these catalysts and under anaerobic conditions, protons are the sole possible electron acceptors, leading to H_2 evolution thus associated with cathodic current.

We measured the current densities by illuminating the biophotoelectrode in an electrochemical cell with a platinum counter electrode but under potential biases of +0.6 and −0.6 V vs an Ag/AgCl reference electrode using monochromatic light of wavelengths 375 (Figure 5A), 420, 470, 505 nm (Figure S5), 530 nm (Figure 5A), 590, and 625 nm (Figure S5). To obtain pure photocurrents (i.e., current occurring solely due to illumination), the dark currents from positive polarization were subtracted from the measured traces.

Photocurrent curves obtained for 420, 470, 505, 590, and 625 nm are shown in the Supporting Information (Figure S5). Here, only data for two wavelengths are presented: 375 nm (high absorbance by cyanobacteria) and 530 nm (low absorbance by cyanobacteria). Figure 5A demonstrates photocurrent densities obtained after subtracting the dark current for 375 and 530 nm illumination. Monochromatic light with wavelength 375 nm produced the maximum photocurrent. For other wavelengths, there is a decreasing trend with longer wavelengths, with slightly higher photocurrents for 505 nm and almost zero photocurrent for 530 nm. This observation aligns well with the absorption spectra of cyanobacteria in the PEDOT/PSS matrix (Figure 2A), demonstrating high absorption for red and blue light and low absorption for green light.

When the BDD/PEDOT/PSS + P6 biophotoelectrode is negatively polarized (−0.6 V), it generates a cathodic photocurrent. In this case, electrons flow in the opposite direction, moving from the BDD electrode to the cyanobacteria embedded in the PEDOT−PSS matrix.

It is worth noting that cathodic photocurrents at negative polarization were recorded even at illumination wavelengths where anodic currents were zero during positive polarization, such as at 530 nm (Figure 4A). This phenomenon may be a consequence of the increase in absorbance at negative voltage, as demonstrated in Figure 3. However, even after being polarized at −0.6 V for an extended period, the absorption of PEDOT/PSS + P6 in the red-yellow (590 and 625 nm) region

https://doi.org/10.1021/acsomega.4c03925
ACS Omega 2024, 9, 32949−32961

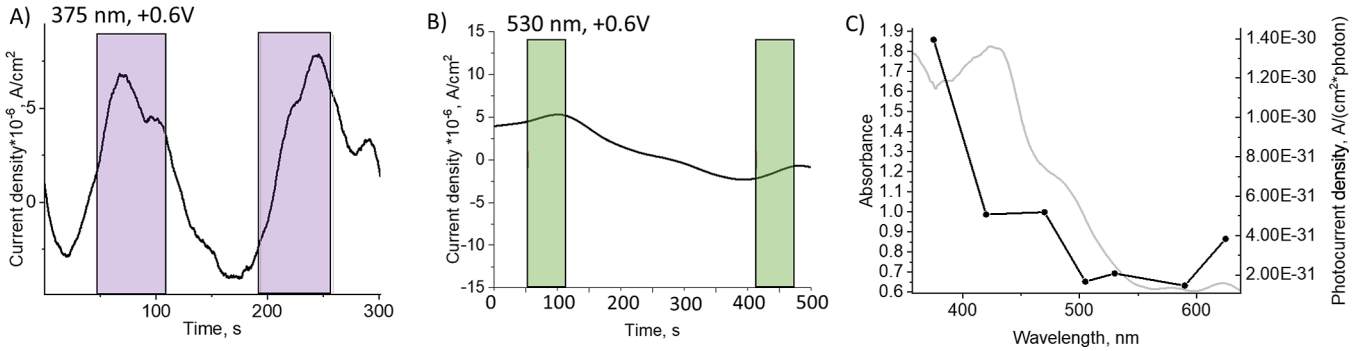

Figure 6. Photocurrents generated by the BDD/agar + P6 biophotoelectrode under illumination by (A) UV light (375 nm) and (B) green light (530 nm) at applied potential biases of +0.6 V, (C) photocurrents produced by the BDD/agar + P6 biophotoelectrode under illumination by monochromatic light at applied potential biases of +0.6 V normalized to photon flux and plotted together with the agar + P6 absorption spectrum for reference. Colored bars designate periods of illumination.

of the visible light spectrum remains lower compared to the blue part of the spectrum (420, 470, and 505 nm). Nevertheless, cathodic photocurrents produced by the negatively polarized PEDOT/PSS + P6 biophotoelectrode when illuminated with red light (680 nm) are almost equivalent to those produced by 360 nm light.

Figure 5B summarizes data on photocurrents generated by PEDOT−PSS-embedded cyanobacteria under +0.6 and −0.6 V potential bias and monochromatic illumination in the visible light range. Correspondence between light absorption and current density generated per photon of incident light can be observed in general. However, cathodic photocurrent density measured at negative polarization for red light (625 nm) is higher than that can be expected from the absorption spectrum. Also chlorophyll absorption feature at the UV-blue region (380 nm) does not find reflection in photocurrent density curve: high light absorption result in low photocurrent density measured. However, when photocurrents were measured for a PEDOT−PSS layer only (i.e., without cyanobacteria), cathodic photocurrent was measured at negative potential bias for UV (375 nm) and red (625 nm) illumination only, whereas anodic photocurrent was obtained for all other wavelengths tested.

At +0.6 V polarization, photocurrents for pure (cell-free) PEDOT/PSS-coated BDD electrodes were significantly higher at wavelengths <500 nm comparing to the biophotoelectrode (Figure S6). Even though PEDOT/PSS is reported not to be photoactive and does not contribute to photocurrent generation in biophotoelectrochemical systems,[75] it may influence the semiconductor photopotential and hence affect produced photocurrents.[53] It indeed may be a possible explanation for the higher anodic photocurrents we measured for cell-free BDD/PEDOT/PSS but as this is beyond the scope of the present study, we did not further pursue this. At negative polarization, cyanobacteria embedded in PEDOT/PSS are responsible to cathodic photocurrent appearance because pure, cell-free PEDOT/PSS on top of BDD displayed a photoanodic response for 400−600 nm range.

As demonstrated here, BDD/PEDOT/PSS + P6 biophotoelectrodes can be utilized as photocathodes and photoanodes in BPV and BPEC cells. Cathodic processes appear to be more efficient, generating higher photocurrents, and they utilize the entire visible spectrum to generate photoelectricity. However, no anodic photocurrent is produced with green illumination, likely because it is poorly absorbed by photosynthetic pigments in cyanobacteria.

To exclude the effect of conductive and electrochromic polymers, we also made biophotoelectrodes with cyanobacteria embedded in the polysaccharide matrix of agar. Figure S7 demonstrates chronoamperometry curves for agar-embedded cyanobacteria with photoresponses to monochromatic illumination designated by colored bars. As can be seen from this figure, the photoresponse is not very consistent: not every illumination period corresponds to rise and fall of current measured, and also some current oscillations are observed without respect to illumination. Furthermore, if we assume that current rise is attributed to electricity generated by photosynthetic microorganisms, the current is of the same order of magnitude as the one measured for PEDOT−PSS, even though at any rate agar is much less conductive in comparison to PEDOT/PSS (Figure S4A). Also, oscillations in current were observed for illuminations of BDD/agar + P6 with green and yellow light (530 and 590 nm) which is not expected according to the "agar + P6" absorption profile.

Addition of the artificial mediator ferricyanide, $[Fe(CN)_6]^{3+}$, has been reported to significantly enhance the current.[76] $[Fe(CN)_6]^{3+}$ accepts electrons from NADPH at the external surface of the cells.[3] In the case of agar-embedded cyanobacteria, the addition of $[Fe(CN)_6]^{3+}$ made the system indeed more conductive (Figure S4A) with values of currents an order of magnitude higher than values of current in the absence of $[Fe(CN)_6]^{3+}$. However, oscillations in current during measurements apparently not related to illumination were also observed (Figure S8). These "photocurrents" were 1 order of magnitude higher comparing to pure agar, and also low currents were observed for green and yellow illumination which could indicate bioderived photocurrent. Such inconsistencies in light response hampers further analysis since it leads to mean square deviation values compared to average values of photocurrent. Figure 6 demonstrates responses in current for the BDD/agar + P6 electrode under +0.6 V potential bias at 375 (A) and 530 (B) nm illumination. Data normalized to light intensities and number of photons are presented in Figure 5, panel C.

In heterogeneous systems like BPEC cells, there is indeed a requirement for a charge carrier at the interface between cyanobacteria and the current collector. The thickness of the film or matrix, in which the cyanobacteria are embedded, can play a significant role in the small current output. When the film becomes too thick, it can impede the efficient diffusion of charge carriers or shuttling molecules to the interface, which can result in decreased photocurrents. Additionally, if the film

https://doi.org/10.1021/acsomega.4c03925
ACS Omega 2024, 9, 32949−32961

becomes too thick, it may lead to the formation of a nonconducting layer of cells, further reducing current output. Therefore, optimizing the film thickness and the overall design of the BPEC is crucial for achieving higher photocurrents and overall performance.

CONCLUSIONS

We have shown the relationship between electrical polarization and the photosynthetic activity of cyanobacteria on BDD substrates. In this, we demonstrated that matrix conductivity plays a key role not only for charge-transfer efficiency but also for a better biological absorbance under polarization conditions. The observed increase in cyanobacterial light absorbance under negative electrical polarization, along with cathodic and anodic photocurrent generation depending on polarization, underscore the importance of investigating the interplay between electrochemical conditions and molecular biological processes in the design of energy-generating technologies that are based on living microorganisms. The ability of cyanobacteria to harness light energy and enhance their light absorbance in response to negative electrical polarizations opens up interesting perspectives for rational biophotocathode design. This knowledge is crucial for the optimization of conditions in the development of more efficient bioelectrochemical systems comprising cyanobacteria and BDD substrates.

ASSOCIATED CONTENT

Supporting Information

The Supporting Information is available free of charge at https://pubs.acs.org/doi/10.1021/acsomega.4c03925.

Additional experimental data: light absorbance spectra of various cyanobacteria cultures, light absorbance spectra derivatives for possible peak position shift determination, data on dark currents of cyanobacteria embedded in various matrices, light absorbance of cyanobacteria free polymer matrices, and photocurrent data (PDF)

AUTHOR INFORMATION

Corresponding Authors

Nikolay Ryzhkov − *Empa. Swiss Federal Laboratories for Materials Science and Technology, Laboratory for High Performance Ceramics, Dübendorf CH-8600, Switzerland*; Email: nikolay.ryzhkov@empa.ch

Artur Braun − *Empa. Swiss Federal Laboratories for Materials Science and Technology, Laboratory for High Performance Ceramics, Dübendorf CH-8600, Switzerland*; orcid.org/0000-0002-6992-7774; Email: artur.braun@alumni.ethz.ch

Authors

Nora Colson − *Empa. Swiss Federal Laboratories for Materials Science and Technology, Laboratory for High Performance Ceramics, Dübendorf CH-8600, Switzerland; Institute for Materials Research (IMO), Hasselt University, Diepenbeek B-3590, Belgium; IMOMEC, IMEC vzw, Diepenbeek B-3590, Belgium*

Essraa Ahmed − *Institute for Materials Research (IMO), Hasselt University, Diepenbeek B-3590, Belgium; IMOMEC, IMEC vzw, Diepenbeek B-3590, Belgium*; orcid.org/0000-0002-9400-5587

Paulius Pobedinskas − *Institute for Materials Research (IMO), Hasselt University, Diepenbeek B-3590, Belgium; IMOMEC, IMEC vzw, Diepenbeek B-3590, Belgium*; orcid.org/0000-0001-8136-5172

Ken Haenen − *Institute for Materials Research (IMO), Hasselt University, Diepenbeek B-3590, Belgium; IMOMEC, IMEC vzw, Diepenbeek B-3590, Belgium*; orcid.org/0000-0001-6711-7367

Paul J. Janssen − *Institute for Nuclear Medical Applications, Belgian Nuclear Research Centre, Mol B-2400, Belgium*

Complete contact information is available at: https://pubs.acs.org/10.1021/acsomega.4c03925

Author Contributions

N.R. set up and carried out the electrochemical and optical spectroscopy experiments and data analysis and written the manuscript. A.B. and P.J.J. envisioned this project, laid out the scientific concept of biophotoelectrochemistry, guided the experimental course, and acquired the funding together with K.H., who provided the platform for semiconductor electrode support. P.P. oversaw the synthesis of the diamond films, supported by E.A. and N.C. All authors have contributed to the finalizing of the results and writing of the manuscript.

Notes

The authors declare no competing financial interest.

ACKNOWLEDGMENTS

This work is financially supported by the Swiss National Science Foundation under project number 200021 × $10^{-189455}$ and Research Foundation Flanders (FWO) grant no. G0D4920N in the framework of "Flanders/Swiss Lead Agency Process: Charge and energy transfer between cyanobacteria and semiconductor electrodes under gamma-irradiation". Financial support by the Special Research Fund (BOF) via the Methusalem NANO network (ref.: BOF08M02) and by the European Space Agency ESA (sustainable hydrogen production in space by radiation hard cyanobacterial biofilms in a photoelectrochemical system using BDD electrodes; OSIP Idea I-2021-00820, contract number 4000137808) are gratefully acknowledged. N.C. is grateful for the Doctoral School Mobility grant (U Hasselt Call 1-2023) and the Frank De Winne Fellowship (sustainable hydrogen production for space applications, # 1SF1423N). The authors thank Ilse Coninx (SCK CEN) for priceless help with cyanobacteria culturing.

REFERENCES

(1) (a) Parmar, A.; Singh, N. K.; Pandey, A.; Gnansounou, E.; Madamwar, D. Cyanobacteria and microalgae: A positive prospect for biofuels. *Bioresour. Technol.* **2011**, *102* (22), 10163−10172. (b) Rosenbaum, M.; He, Z.; Angenent, L. T. Light energy to bioelectricity: photosynthetic microbial fuel cells. *Curr. Opin. Biotechnol.* **2010**, *21* (3), 259−264.

(2) Braun, A.; Boudoire, F.; Bora, D. K.; Faccio, G.; Hu, Y.; Kroll, A.; Mun, B. S.; Wilson, S. T. Biological components and bioelectronic interfaces of water splitting photoelectrodes for solar hydrogen production. *Chem.—Eur. J.* **2015**, *21* (11), 4188−4199.

(3) Shlosberg, Y.; Schuster, G.; Adir, N. Harnessing photosynthesis to produce electricity using cyanobacteria, green algae, seaweeds and plants. *Front. Plant Sci.* **2022**, *13*, 955843.

(4) Kato, Y.; Inabe, K.; Hidese, R.; Kondo, A.; Hasunuma, T. Metabolomics-based engineering for biofuel and bio-based chemical production in microalgae and cyanobacteria: A review. *Bioresour. Technol.* **2022**, *344*, 126196.

(5) Arias, D. M.; García, J.; Uggetti, E. Production of polymers by cyanobacteria grown in wastewater: Current status, challenges and future perspectives. *New Biotechnol.* **2020**, *55*, 46−57.
(6) (a) Pescheck, M.; Schweizer, A.; Bláha, L. Innovative electrochemical biosensor for toxicological investigations on algae and cyanobacteria. *Bioelectrochemistry* **2022**, *143*, 107926. (b) Ameen, F.; Hamidian, Y.; Mostafazadeh, R.; Darabi, R.; Erk, N.; Islam, M. A.; Orfali, R. A novel atropine electrochemical sensor based on silver nano particle-coated Spirulina platensis multicellular blue-green microalga. *Chemosphere* **2023**, *324*, 138180.
(7) Mapstone, L. J.; Leite, M. N.; Purton, S.; Crawford, I. A.; Dartnell, L. Cyanobacteria and microalgae in supporting human habitation on Mars. *Biotechnol. Adv.* **2022**, *59*, 107946.
(8) (a) Polyakov, Y. S.; Musaev, I.; Polyakov, S. V. Closed bioregenerative life support systems: Applicability to hot deserts. *Adv. Space Res.* **2010**, *46* (6), 775−786. (b) Braun, A. *Quantum Electrodynamics of Photosynthesis—Mathematical Description of Light, Life and Matter*; De Gruyter, 2020.
(9) Ferrazzano, G. F.; Papa, C.; Pollio, A.; Ingenito, A.; Sangianantoni, G.; Cantile, T. Cyanobacteria and Microalgae as Sources of Functional Foods to Improve Human General and Oral Health. *Molecules* **2020**, *25* (21), 5164.
(10) Chittora, D.; Meena, M.; Barupal, T.; Swapnil, P.; Sharma, K. Cyanobacteria as a source of biofertilizers for sustainable agriculture. *Biochem. Biophys. Rep.* **2020**, *22*, 100737.
(11) Wangpraseurt, D.; You, S. T.; Sun, Y. Z.; Chen, S. C. Biomimetic 3D living materials powered by microorganisms. *Trends Biotechnol.* **2022**, *40* (7), 843−857.
(12) (a) Keller, R.; Goli, K.; Porter, W.; Alrabaa, A.; Jones, J. A. Cyanobacteria and Algal-Based Biological Life Support System (BLSS) and Planetary Surface Atmospheric Revitalizing Bioreactor Brief Concept Review. *Life-Basel* **2023**, *13* (3), 816. (b) Ross, B.; Haussener, S.; Brinkert, K. Assessment of the technological viability of photoelectrochemical devices for oxygen and fuel production on Moon and Mars. *Nat. Commun.* **2023**, *14* (1), 3141. (c) Santomartino, R.; Averesch, N. J. H.; Bhuiyan, M.; Cockell, C. S.; Colangelo, J.; Gumulya, Y.; Lehner, B.; Lopez-Ayala, I.; McMahon, S.; Mohanty, A.; et al. Toward sustainable space exploration: a roadmap for harnessing the power of microorganisms. *Nat. Commun.* **2023**, *14* (1), 1391.
(13) Ye, J.; Hu, A. D.; Ren, G. P.; Chen, M.; Zhou, S. G.; He, Z. Biophotoelectrochemistry for renewable energy and environmental applications. *Iscience* **2021**, *24* (8), 102828.
(14) McCormick, A. J.; Bombelli, P.; Bradley, R. W.; Thorne, R.; Wenzel, T.; Howe, C. J. Biophotovoltaics: oxygenic photosynthetic organisms in the world of bioelectrochemical systems (vol 8, pg 1092, 2015). *Energy Environ. Sci.* **2015**, *8* (5), 1627.
(15) Liu, L.; Choi, S. Enhanced biophotoelectricity generation in cyanobacterial biophotovoltaics with intracellularly biosynthesized gold nanoparticles. *J. Power Sources* **2021**, *506*, 230251.
(16) Torquato, L. D. D.; Grattieri, M. Photobioelectrochemistry of intact photosynthetic bacteria: Advances and future outlook. *Curr. Opin. Electrochem.* **2022**, *34*, 101018.
(17) Lai, B.; Schneider, H.; Tschörtner, J.; Schmid, A.; Krömer, J. O. Technical-scale biophotovoltaics for long-term photo-current generation from Synechocystis sp. PCC6803. *Biotechnol. Bioeng.* **2021**, *118* (7), 2637−2648.
(18) (a) Balskus, E. P.; Walsh, C. T. The Genetic and Molecular Basis for Sunscreen Biosynthesis in Cyanobacteria. *Science* **2010**, *329* (5999), 1653−1656. (b) Dittmann, E.; Neilan, B. A.; Börner, T. Molecular biology of peptide and polyketide biosynthesis in cyanobacteria. *Appl. Microbiol. Biotechnol.* **2001**, *57* (4), 467−473. (c) Averesch, N. J. H. Choice of Microbial System for In-Situ Resource Utilization on Mars. *Front Astron Space* **2021**, *8*, 700370.
(19) Saper, G.; Kallmann, D.; Conzuelo, F.; Zhao, F. Y.; Tóth, T. N.; Liveanu, V.; Meir, S.; Szymanski, J.; Aharoni, A.; Schuhmann, W.; et al. Live cyanobacteria produce photocurrent and hydrogen using both the respiratory and photosynthetic systems. *Nat. Commun.* **2018**, *9*, 2168.
(20) Nowicka-Krawczyk, P.; Mühlsteinová, R.; Hauer, T. Detailed characterization of the Arthrospira type species separating commercially grown taxa into the new genus Limnospira (Cyanobacteria). *Sci. Rep.* **2019**, *9*, 694.
(21) Barone, G. D.; Cernava, T.; Ullmann, J.; Liu, J.; Lio, E.; Germann, A. T.; Nakielski, A.; Russo, D. A.; Chavkin, T.; Knufmann, K.; et al. Recent developments in the production and utilization of photosynthetic microorganisms for food applications. *Heliyon* **2023**, *9* (4), No. e14708.
(22) Chin, J. C.; Khor, W. H.; Ng, F. L.; Chong, W. W. F.; Wu, Y. T.; Kang, H. S. Effects of anode materials in electricity generation of microalgal-biophotovoltaic system—part II: Free-floating microalgae in aeration mode. *Mater. Today: Proc.* **2022**, *65*, 2992−2999.
(23) Bombelli, P.; Zarrouati, M.; Thorne, R. J.; Schneider, K.; Rowden, S. J. L.; Ali, A.; Yunus, K.; Cameron, P. J.; Fisher, A. C.; Wilson, D. I.; et al. Surface morphology and surface energy of anode materials influence power outputs in a multi-channel mediatorless bio-photovoltaic (BPV) system. *Phys. Chem. Chem. Phys.* **2012**, *14* (35), 12221−12229.
(24) Bombelli, P.; Savanth, A.; Scarampi, A.; Rowden, S. J. L.; Green, D. H.; Erbe, A.; Årstol, E.; Jevremovic, I.; Hohmann-Marriott, M. F.; Trasatti, S. P.; et al. Powering a microprocessor by photosynthesis. *Energy Environ. Sci.* **2022**, *15* (6), 2529−2536.
(25) Flemming, H. C.; Wingender, J.; Szewzyk, U.; Steinberg, P.; Rice, S. A.; Kjelleberg, S. Biofilms: an emergent form of bacterial life. *Nat. Rev. Microbiol.* **2016**, *14* (9), 563−575.
(26) Buesen, D.; Hoefer, T.; Zhang, H.; Plumere, N. A kinetic model for redox-active film based biophotoelectrodes. *Faraday Discuss.* **2019**, *215* (0), 39−53.
(27) (a) Krujatz, F.; Lode, A.; Brüggemeier, S.; Schütz, K.; Kramer, J.; Bley, T.; Gelinsky, M.; Weber, J. Green bioprinting: Viability and growth analysis of microalgae immobilized in 3D-plotted hydrogels versus suspension cultures. *Eng. Life Sci.* **2015**, *15* (7), 678−688. (b) Ortega, J. S.; Corrales-Orovio, R.; Ralph, P.; Egaña, J. T.; Gentile, C. Photosynthetic microorganisms for the oxygenation of advanced 3D bioprinted tissues*. *Acta Biomater.* **2023**, *165*, 180−196.
(28) (a) Sawa, M.; Fantuzzi, A.; Bombelli, P.; Howe, C. J.; Hellgardt, K.; Nixon, P. J. Electricity generation from digitally printed cyanobacteria. *Nat. Commun.* **2017**, *8*, 1327. (b) Lee, H.; Hyun, J. Biophotovoltaic living hydrogel of an ion-crosslinked carboxymethylated cellulose nanofiber/alginate. *Carbohydr. Polym.* **2023**, *321*, 121299. (c) Caldwell, G. S.; In-na, P.; Hart, R.; Sharp, E.; Stefanova, A.; Pickersgill, M.; Walker, M.; Unthank, M.; Perry, J.; Lee, J. G. M. Immobilising Microalgae and Cyanobacteria as Biocomposites: New Opportunities to Intensify Algae Biotechnology and Bioprocessing. *Energies* **2021**, *14* (9), 2566.
(29) Ng, F. L.; Phang, S. M.; Periasamy, V.; Yunus, K.; Fisher, A. C. Enhancement of Power Output by using Alginate Immobilized Algae in Biophotovoltaic Devices. *Sci. Rep.* **2017**, *7* (1), 16237.
(30) Hazzan, O. O.; Zhao, B. Y.; Xiao, Y. Strategies for Enhancing Extracellular Electron Transfer in Environmental Biotechnology: A Review. *Appl. Sci.* **2023**, *13* (23), 12760.
(31) Hernandez, M. E.; Newman, D. K. Extracellular electron transfer. *Cell. Mol. Life Sci.* **2001**, *58* (11), 1562−1571.
(32) (a) Mouhib, M.; Antonucci, A.; Reggente, M.; Amirjani, A.; Gillen, A. J.; Boghossian, A. A. Enhancing bioelectricity generation in microbial fuel cells and biophotovoltaics using nanomaterials. *Nano Res.* **2019**, *12* (9), 2184−2199. (b) Reggente, M.; Politi, S.; Antonucci, A.; Tamburri, E.; Boghossian, A. A. Design of Optimized PEDOT-Based Electrodes for Enhancing Performance of Living Photovoltaics Based on Phototropic Bacteria. *Adv. Mater. Technol.* **2020**, *5* (3), 1900931.
(33) (a) Pleskov, Y. V. Electrochemistry of diamond: A review. *Russ. J. Electrochem.* **2002**, *38* (12), 1275−1291. (b) Luong, J. H. T.; Male, K. B.; Glennon, J. D. Boron-doped diamond electrode: synthesis, characterization, functionalization and analytical applications. *Analyst* **2009**, *134* (11), 1965.
(34) (a) Taylor, A. C.; Vagaska, B.; Edgington, R.; Hébert, C.; Ferretti, P.; Bergonzo, P.; Jackman, R. B. Biocompatibility of

https://doi.org/10.1021/acsomega.4c03925
ACS Omega 2024, 9, 32949−32961

nanostructured boron doped diamond for the attachment and proliferation of human neural stem cells. *J. Neural Eng.* **2015**, *12* (6), 066016. (b) Garrett, D. J.; Saunders, A. L.; McGowan, C.; Specks, J.; Ganesan, K.; Meffin, H.; Williams, R. A.; Nayagam, D. A. X. In vivo biocompatibility of boron doped and nitrogen included conductive-diamond for use in medical implants. *J. Biomed. Mater. Res., Part B* **2016**, *104* (1), 19−26.

(35) (a) Einaga, Y. Boron-Doped Diamond Electrodes: Fundamentals for Electrochemical Applications. *Acc. Chem. Res.* **2022**, *55* (24), 3605−3615. (b) Rycewicz, M.; Nosek, A.; Shin, D. H.; Ficek, M.; Buijnsters, J. G.; Bogdanowicz, R. The effect of boron concentration on the electrical, morphological and optical properties of boron-doped nanocrystalline diamond sheets: Tuning the diamond-on-graphene vertical junction. *Diamond Relat. Mater.* **2022**, *128*, 109225. (c) Kuang, P. L.; Natsui, K.; Feng, C. P.; Einaga, Y. Electrochemical reduction of nitrate on boron-doped diamond electrodes: Effects of surface termination and boron-doping level. *Chemosphere* **2020**, *251*, 126364.

(36) (a) Macpherson, J. V. The Use of Conducting Diamond in Electrochemistry. *Electrochemistry of Carbon Electrodes*; *Advances in Electrochemical Sciences and Engineering*; John Wiley & Sons, 2016; pp 163−210. (b) Macpherson, J. V. A practical guide to using boron doped diamond in electrochemical research. *Phys. Chem. Chem. Phys.* **2015**, *17* (5), 2935−2949. (c) Wallny, R. S.; Cindro, V.; Dolenc, I.; Frais-Kolbl, H.; Mikuz, M.; Niegl, M.; Pernegger, H.; Trischuk, W.; Weilhammer, P.; Zavrtanik, M.; et al. Status of diamond detectors and their high energy physics application. *Nucl. Instrum. Methods* **2007**, *582* (3), 824−828. (d) Panizza, M.; Cerisola, G. Application of diamond electrodes to electrochemical processes. *Electrochim. Acta* **2005**, *51* (2), 191−199.

(37) Szewczyk, S.; Bialek, R.; Burdzinski, G.; Gibasiewicz, K. Photovoltaic activity of electrodes based on intact photosystem I electrodeposited on bare conducting glass. *Photosynth. Res.* **2020**, *144* (1), 1−12.

(38) Pinhassi, R. I.; Kallmann, D.; Saper, G.; Dotan, H.; Linkov, A.; Kay, A.; Liveanu, V.; Schuster, G.; Adir, N.; Rothschild, A. Hybrid bio-photo-electro-chemical cells for solar water splitting. *Nat. Commun.* **2016**, *7*, 12552.

(39) Zimmermann, U.; Pilwat, G.; Beckers, F.; Riemann, F. Effects of External Electrical Fields on Cell-Membranes. *Bioelectrochem. Bioenerg.* **1976**, *3* (1), 58−83.

(40) Wege, S. Plants Increase Photosynthesis Efficiency by Lowering the Proton Gradient across the Thylakoid Membrane. *Plant Physiol.* **2020**, *182* (4), 1812−1813.

(41) Cruz, J. A.; Sacksteder, C. A.; Kanazawa, A.; Kramer, D. M. Contribution of electric field ($\Delta\psi$) to steady-state transthylakoid proton motive force in vitro and in vivo.: Control of parsing into $\Delta\psi$ and ΔpH by ionic strength. *Biochemistry* **2001**, *40* (5), 1226−1237.

(42) Shlosberg, Y.; Schuster, G.; Adir, N. Harnessing photosynthesis to produce electricity using cyanobacteria, green algae, seaweeds and plants. *Front. Plant Sci.* **2022**, *13*, 955843.

(43) Degrooth, B. G.; Vangorkom, H. J. External Electric-Field Effects on Prompt and Delayed Fluorescence in Chloroplasts. *Biochim. Biophys. Acta* **1981**, *635* (3), 445−456.

(44) Zhu, X.; Yates, M. D.; Hatzell, M. C.; Ananda Rao, H.; Saikaly, P. E.; Logan, B. E. Microbial community composition is unaffected by anode potential. *Environ. Sci. Technol.* **2014**, *48* (2), 1352−1358.

(45) Gamero-Quijano, A.; Herzog, G.; Scanlon, M. D. Bioelectrochemistry of Cytochrome c in a closed bipolar electrochemical cell. *Electrochem. Commun.* **2019**, *109*, 106600.

(46) Khorobrykh, S.; Havurinne, V.; Mattila, H.; Tyystjärvi, E. Oxygen and ROS in Photosynthesis. *Plants-Basel* **2020**, *9* (1), 91.

(47) Pobedinskas, P.; Degutis, G.; Dexters, W.; Janssen, W.; Janssens, S. D.; Conings, B.; Ruttens, B.; D'Haen, J.; Boyen, H. G.; Hardy, A.; et al. Surface plasma pretreatment for enhanced diamond nucleation on AlN. *Appl. Phys. Lett.* **2013**, *102* (20), 201609.

(48) Yadav, A.; Monsieurs, P.; Misztak, A.; Waleron, K.; Leys, N.; Cuypers, A.; Janssen, P. J. Helical and linear morphotypes of Arthrospira sp. PCC 8005 display genomic differences and respond differently to ^{60}Co gamma irradiation. *Eur. J. Phycol* **2020**, *55* (2), 129−146.

(49) Zarrouk, C. *Contribution à l'étude d'une Cyanophycée: Influence de Divers Facteurs Physiques et Chimiques sur la Croissance et la Photosynthèse de Spirulina Maxima (Setch et Gardner) Geitler*; Universite de Paris: Paris, 1966

(50) Cogne, G.; Lehmann, B.; Dussap, C. G.; Gros, J. B. Uptake of macrominerals and trace elements by the cyanobacterium Spirulina platensis (Arthrospira platensis PCC 8005) under photoautotrophic conditions: culture medium optimization. *Biotechnol. Bioeng.* **2003**, *81* (5), 588−593.

(51) Kandilian, R.; Jesus, B.; Legrand, J.; Pilon, L.; Pruvost, J. Light transfer in agar immobilized microalgae cell cultures. *J. Quant. Spectrosc. Radiat.* **2017**, *198*, 81−92.

(52) Wolfe, K. D.; Gargye, A.; Mwambutsa, F.; Than, L.; Cliffel, D. E.; Jennings, G. K. Layer-by-Layer Assembly of Photosystem I and PEDOT:PSS Biohybrid Films for Photocurrent Generation. *Langmuir* **2021**, *37* (35), 10481−10489.

(53) Jing, J.; Wang, X.; Chen, Z.; Feng, C.; Ma, L.; Hou, J.; Xu, L.; Sun, M. PEDOT:PSS helps to reveal the decisive role of photocurrent and photopotential on the photoinduced cathodic protection performance. *J. Electroanal. Chem.* **2023**, *943*, 117607.

(54) (a) Strítesky, S.; Marková, A.; Vítecek, J.; Safaríková, E.; Hrabal, M.; Kubác, L.; Kubala, L.; Weiter, M.; Vala, M. Printing inks of electroactive polymer PEDOT:PSS: The study of biocompatibility, stability, and electrical properties. *J. Biomed Mater. Res. A* **2018**, *106* (4), 1121−1128. (b) Yang, T.; Yang, M.; Xu, C.; Yang, K.; Su, Y.; Ye, Y.; Dou, L.; Yang, Q.; Ke, W.; Wang, B.; et al. PEDOT:PSS hydrogels with high conductivity and biocompatibility for in situ cell sensing. *J. Mater. Chem. B* **2023**, *11* (14), 3226−3235.

(55) Saini, D. K.; Pabbi, S.; Shukla, P. Cyanobacterial pigments: Perspectives and biotechnological approaches. *Food Chem. Toxicol.* **2018**, *120*, 616−624.

(56) Luimstra, V. M.; Schuurmans, J. M.; Verschoor, A. M.; Hellingwerf, K. J.; Huisman, J.; Matthijs, H. C. P. Blue light reduces photosynthetic efficiency of cyanobacteria through an imbalance between photosystems I and II. *Photosynth. Res.* **2018**, *138* (2), 177−189.

(57) (a) Ruiz-Verdú, A.; Simis, S. G. H.; de Hoyos, C.; Gons, H. J.; Peña-Martínez, R. An evaluation of algorithms for the remote sensing of cyanobacterial biomass. *Remote Sens Environ* **2008**, *112* (11), 3996−4008. (b) Tebbs, E. J.; Remedios, J. J.; Harper, D. M. Remote sensing of chlorophyll-a as a measure of cyanobacterial biomass in Lake Bogoria, a hypertrophic, saline−alkaline, flamingo lake, using Landsat ETM+. *Remote Sens Environ* **2013**, *135*, 92−106.

(58) Shevela, D.; Kern, J. F.; Govindjee, G.; Messinger, J. Solar energy conversion by photosystem II: principles and structures. *Photosynth. Res.* **2023**, *156* (3), 279−307.

(59) Rochaix, J. D. Regulation of photosynthetic electron transport. *Biochim. Biophys. Acta, Bioenerg.* **2011**, *1807* (3), 375−383.

(60) Bianchetti, R.; De Luca, B.; de Haro, L. A.; Rosado, D.; Demarco, D.; Conte, M.; Bermudez, L.; Freschi, L.; Fernie, A. R.; Michaelson, L. V.; et al. Phytochrome-Dependent Temperature Perception Modulates Isoprenoid Metabolism. *Plant Physiol.* **2020**, *183* (3), 869−882.

(61) (a) Degrooth, B. G.; Vangorkom, H. J.; Meiburg, R. F. Electrochromic Absorbance Changes in Spinach-Chloroplasts Induced by an External Electrical-Field. *Biochim. Biophys. Acta* **1980**, *589* (2), 299−314. (b) Frese, R. N.; Palacios, M. A.; Azzizi, A.; van Stokkum, I. H. M.; Kruip, J.; Rögner, M.; Karapetyan, N. V.; Schlodder, E.; van Grondelle, R.; Dekker, J. P. Electric field effects on red chlorophylls, β-carotenes and P700 in cyanobacterial Photosystem I complexes. *Biochim. Biophys. Acta, Bioenerg.* **2002**, *1554* (3), 180−191.

(62) Saini, D. K.; Pabbi, S.; Shukla, P. Cyanobacterial pigments: Perspectives and biotechnological approaches. *Food Chem. Toxicol.* **2018**, *120*, 616−624.

(63) (a) Do, M.; Park, C.; Bae, S.; Kim, J.; Kim, J. H. Design of highly stable and solution-processable electrochromic devices based

https://doi.org/10.1021/acsomega.4c03925
ACS Omega 2024, 9, 32949−32961

on PEDOT:PSS. *Org. Electron.* **2021**, *93*, 106106. (b) WangZhiqi Wang, Z. R. L.; Liu, R. PEDOT:PSS-based electrochromic materials for flexible and stretchable devices. *Materials Today Electronics* **2023**, *4*, 100036.

(64) (a) Ehrenberg, B.; Farkas, D. L.; Fluhler, E. N.; Lojewska, Z.; Loew, L. M. Membrane potential induced by external electric field pulses can be followed with a potentiometric dye. *Biophys. J.* **1987**, *51* (5), 833−837. (b) Escobar, J. F.; Vaca-González, J. J.; Guevara, J. M.; Garzón-Alvarado, D. A. Effect of magnetic and electric fields on plasma membrane of single cells: A computational approach. *Eng. Rep.* **2020**, *2* (2), No. e12125.

(65) (a) Blumenthal, R.; Kempf, C.; Van Renswoude, J.; Weinstein, J. N.; Klausner, R. D. Voltage-dependent orientation of membrane proteins. *J. Cell. Biochem.* **1983**, *22* (1), 55−67. (b) Jiang, Z.; You, L.; Dou, W.; Sun, T.; Xu, P. Effects of an Electric Field on the Conformational Transition of the Protein: A Molecular Dynamics Simulation Study. *Polymers* **2019**, *11* (2), 282. (c) Ilieva, S.; Cheshmedzhieva, D.; Dudev, T. Electric field influence on the helical structure of peptides: insights from DFT/PCM computations. *Phys. Chem. Chem. Phys.* **2019**, *21* (29), 16198−16206. (d) Sinelnikova, A.; Mandl, T.; Agelii, H.; Granas, O.; Marklund, E. G.; Caleman, C.; De Santis, E. Protein orientation in time-dependent electric fields: orientation before destruction. *Biophys. J.* **2021**, *120* (17), 3709−3717. (e) Ojeda-May, P.; Garcia, M. E. Electric Field-Driven Disruption of a Native β-Sheet Protein Conformation and Generation of a Helix-Structure. *Biophys. J.* **2010**, *99* (2), 595−599. (f) Zhang, X. C.; Li, H. Interplay between the electrostatic membrane potential and conformational changes in membrane proteins. *Protein Sci.* **2019**, *28* (3), 502−512.

(66) Balevicius, V., Jr.; Fox, K. F.; Bricker, W. P.; Jurinovich, S.; Prandi, I. G.; Mennucci, B.; Duffy, C. D. P. Fine control of chlorophyll-carotenoid interactions defines the functionality of light-harvesting proteins in plants. *Sci. Rep.* **2017**, *7* (1), 13956.

(67) Grudzinski, W.; Krupa, Z.; Garstka, M.; Maksymiec, W.; Swartz, T. E.; Gruszecki, W. I. Conformational rearrangements in light-harvesting complex II accompanying light-induced chlorophyll a fluorescence quenching. *Biochim. Biophys. Acta* **2002**, *1554* (1−2), 108−117.

(68) Zeng, L.; Liao, Z.; Wang, X. H. Geometry Effects on Light-Harvesting Complex's Light Absorption and Energy Transfer in Purple Bacteria. *Photochem. Photobiol.* **2019**, *95* (6), 1352−1359.

(69) Bollella, P.; Melman, A.; Katz, E. Electrochemically Generated Interfacial pH Change: Application to Signal-Triggered Molecule Release. *ChemElectroChem.* **2020**, *7* (16), 3386−3403.

(70) (a) Uffen, R. L. Influence of pH, O2, and temperature on the absorption properties of the secondary light-harvesting antenna in members of the family Rhodospirillaceae. *J. Bacteriol.* **1985**, *163* (3), 943−950. (b) Kim, E.; Watanabe, A.; Sato, R.; Okajima, K.; Minagawa, J. pH-Responsive Binding Properties of Light-Harvesting Complexes in a Photosystem II Supercomplex Investigated by Thermodynamic Dissociation Kinetics Analysis. *J. Phys. Chem. Lett.* **2019**, *10* (13), 3615−3620.

(71) Pinhassi, R. I.; Kallmann, D.; Saper, G.; Dotan, H.; Linkov, A.; Kay, A.; Liveanu, V.; Schuster, G.; Adir, N.; Rothschild, A. Hybrid bio-photo-electro-chemical cells for solar water splitting. *Nat. Commun.* **2016**, *7*, 12552.

(72) Zhao, F. Y.; Conzuelo, F.; Hartmann, V.; Li, H. G.; Nowaczyk, M. M.; Plumeré, N.; Rögner, M.; Schuhmann, W. Light Induced H_2 Evolution from a Biophotocathode Based on Photosystem 1 − Pt Nanoparticles Complexes Integrated in Solvated Redox Polymers Films. *J. Phys. Chem. B* **2015**, *119* (43), 13726−13731.

(73) Aoyama, K.; Uemura, I.; Miyake, J.; Asada, Y. Fermentative metabolism to produce hydrogen gas and organic compounds in a cyanobacterium, Spirulina platensis. *J. Ferment. Bioeng.* **1997**, *83* (1), 17−20.

(74) Dutta, D.; De, D.; Chaudhuri, S.; Bhattacharya, S. K. Hydrogen production by Cyanobacteria. *Microb. Cell Fact.* **2005**, *4*, 36.

(75) Nabhan, M. A.; Batista, C. A. S.; Cliffel, D. E.; Jennings, G. K. Spin Coating Photoactive Photosystem I-PEDOT:PSS Composite Films. *ACS Appl. Polym. Mater.* **2023**, *5* (5), 3278−3288.

(76) Shlosberg, Y.; Toth, T. N.; Eichenbaum, B.; Keysar, L.; Schuster, G.; Adir, N. Electron Mediation and Photocurrent Enhancement in Dunalliela salina Driven Bio-Photo Electrochemical Cells. *Catalysts* **2021**, *11* (10), 1220.

https://doi.org/10.1021/acsomega.4c03925
ACS Omega 2024, 9, 32949−32961